ELSEVIER

Biophysical Chemistry 109 (2004) 157–167

Biophysical Chemistry

www.elsevier.com/locate/bpc

Bohr-effect and buffering capacity of hemocyanin from the tarantula *E. californicum*

Nadja Hellmann*

Institute for Molecular Biophysics, University of Mainz, Jakob-Welder-Weg 26, 55128 Mainz, Germany

Received 4 February 2003; received in revised form 29 October 2003; accepted 29 October 2003

Abstract

A previous report showed that binding of oxygen to the 24-meric hemocyanin from *E. californicum* does not correlate linearly with the release of protons as known from hemoglobin. However, this unusual complex phenomenological observation could not be explained at that time. Here, I present a full analysis of the thermodynamic coupling between protons and oxygen for the 24-meric tarantula hemocyanin in Ringer-solution based on the Nested-MWC-model. A strategy is presented which allows to reduce the number of free parameters when fitting the model to the data by including explicitly the equilibrium constants for binding of protons to the different conformations. The results show that the Nested-MWC-model presents a good description of the cooperative and allosteric properties of spider hemocyanin also under physiological conditions and additional constraints imposed by proton-binding data. The analysis allowed to estimate the average number of allosteric proton-binding sites per subunit and the corresponding pK for each conformation. Furthermore, an estimate of the number and affinity of proton buffering binding sites could be given. Approximately 80% of all proton-binding sites are non-allosteric buffering binding sites. The results obtained in this study allow to predict the relative contribution of the four different conformations under conditions found in vivo. The conformational distribution indicates that the conformation with the highest proton affinity (tR) might be important for the proton transport in the hemolymph.

Keywords: Nested-MWC-model; Bohr-effect; Allostery; Hemocyanin; Proton binding

1. Introduction

Hemocyanins are respiratory proteins found in the hemolymph of some molluscs and arthropods. In arthropods these large protein complexes occur as multiples of hexamers such as 1×6, 2×6, 4×6, 6×6, 8×6 [1–4]. Each monomeric subunit contains one oxygen-binding site. The oxygen-binding properties of hemocyanins are modulated by a number of organic and inorganic effectors [5–14]. Among these, protons play a dominant role, since pH changes occur in response to both environmental and metabolic factors. Thus, for most hemocyanins the Bohr-effect was experimentally determined [15–22]. The slope of log p_{50} vs. log pH yields the Bohr-coefficient as a measure of the influence of protons on the oxygen-binding properties. Usually, a negative Bohr-coefficient is

*Tel.: +49-6131-392-3565; fax: +49-6131-392-3557.
E-mail address: nhellman@uni-mainz.de (N. Hellmann).

0301-4622/04/$ - see front matter © 2003 Elsevier B.V. All rights reserved.
doi:10.1016/j.bpc.2003.10.031

found (for an overview see Ref. [15]). Protons are the only effectors found so far, which increase the p50 of hemocyanins, all others decrease this value.

The cooperative oxygen binding of a number of hemocyanins was well explained in terms of concerted models such as the MWC, the three-state MWC or the Nested-MWC-model [21,23–28]. Common to all concerted models is that different conformations are postulated, which are characterised by their specific ligand- and effector-binding constants. Presence of ligand or effector induces a shift of the conformational distribution. Thus, the allosteric equilibrium constants as obtained from the analysis of ligand-binding curves are a function of the effector concentration. The 2×6-meric hemocyanin from *H. americanus* and the 4×6-meric hemocyanin from *E. californicum* may serve as a typical example. Here, it was shown that the pH value only influences the value of the allosteric equilibrium constants in the framework of the Nested-MWC-model, while the oxygen-binding constants for the four conformations are independent on pH ranging from 7.0 to 8.2 [26].

Due to the thermodynamic coupling between protons and oxygen, the observed change in oxygen saturation upon change in proton concentration necessarily implies that a change in oxygen concentration leads to a change in proton saturation. However, only for one hemocyanin, the binding and release of protons were reported, the hemocyanin from *E. californicum* [29]. In contrast to studies performed on hemoglobins [30], the proton-binding behaviour of this hemocyanin is characterised by a non-monotonous response to the change in oxygen concentration. No attempt was made so far to interpret these data in the framework of an allosteric model. Here, I provide a full analysis of the thermodynamic coupling between protons and oxygen for the 4×6-meric hemocyanin from *E. californicum* based on the Nested-MWC-model. Thus, for the first time for any hemocyanin, the proton-binding properties of the different conformations relevant for establishing cooperativity are characterised and the conformational distribution of spider hemocyanin for physiological conditions is predicted.

2. Experimental

Hemocyanin from the spider *E. californicum* was obtained and purified as described elsewhere [31]. Measurements were performed in solution containing physiological ion composition (210 mM NaCl, 2.6 mM KCl, 0.4 mM $MgCl_2$, 4.2 mM $CaCl_2$, referred to as Ringer-solution further on) in absence of additional buffering system.

Proton release and uptake data were taken from [29]. Oxygen-binding curves were determined employing the change in the absorbance at 339 nm using the same instrument as used for the measurement of proton release and uptake. Protein concentrations ranged between 25 and 45 mg ml^{-1}. No higher aggregates than the 4×6-mers were detected in significant concentrations based on analytical ultracentrifugation and size exclusion chromatography.

Buffer capacity measurements were performed under oxygenated conditions, by titrating 0.1 M NaOH solution in small increments and measuring the pH after equilibration. Since the solution was equilibrated with air, the buffering capacity was corrected for the contribution of bicarbonate based on a partition coefficient of 0.04 mM $Torr^{-1}$ and a pK of 6.14. The concentration of hemocyanin was 37 mg ml^{-1}.

3. Theory

The oxygen-binding properties of hemocyanin can well be explained based on the concerted MWC-model or variants like the Nested-MWC-model or a hybrid-model [21,23–28]. Although this type of model is characterised by a relatively small number of free parameters compared to sequential models, numerical coupling between pairs of parameters frequently occurs, leading to a significant uncertainty in the values of the corresponding parameters. This versatility can be reduced when different types of data like oxygen- and effector-binding data are analysed simultaneously. For concerted models the effector-binding constants can be included explicitly into the function describing ligand binding via the allosteric equilibrium constants. The values for the effector-binding constants obtained by analysing oxygen-

binding data at different effector concentrations can then be compared with results obtained by analysing effector-binding data directly. This strategy is followed in the present analysis of the allosteric effect of protons on the oxygen-binding properties of 24-meric hemocyanin from *E. californicum*.

3.1. General form of the Nested-MWC-model

The saturation of hemocyanin with oxygen and protons is described in terms of the Nested-MWC-model (Fig. 1). The general binding polynomial for a 2×12-mer such as the hemocyanin from *E. californicum*, including explicitly the proton-binding constants is given by

$$P=(QrR^{12m}\mathrm{P}rR^{12}+lR^{oo}QtR^{12m}PtR^{12})^2$$

$$+\Lambda^{oo}(QrT^{12m}\mathrm{P}rT^{12}+lT^{oo}QtT^{12m}PtT^{12})^2$$

$$\Lambda^{oo}=L^{oo}\frac{(1+lR^{oo})^2}{(1+lT^{oo})^2}$$

$$P_{\alpha\beta}=1+k_{\alpha\beta}x \quad Q_{\alpha\beta}=1+z_{\alpha\beta}y$$

$$\alpha\beta=tT,\ rT,\ rR,\ tR \tag{1}$$

The oxygen concentration is given by x, the proton concentration by y. The oxygen-binding constants for the four conformations are denoted by *ktT*, *ktR*, *krR* and *krT*, the proton-binding constants by *ztT*, *ztR*, *zrR* and *zrT* and the equilibrium between the four conformations in absence of oxygen and protons by L^{oo}, lT^{oo}, lR^{oo} with

$$L^{oo}=\frac{[T_{oo}]}{[R_{oo}]} \quad lT^{oo}=\frac{[tT_{oo}]}{[rT_{oo}]} \quad lR^{oo}=\frac{[tR_{oo}]}{[rR_{oo}]} \tag{2}$$

Here, the brackets denote the concentration of allosteric units in the different conformations: [*tT*], [*rT*], [*tR*] and [*rR*] for the 12-meric allosteric unit, and [*T*], [*R*] for the 24-meric allosteric unit (see also Fig. 1).

The average number of proton-binding sites per subunit is denoted by m. The proton-binding constants and the stoichiometry m have to be regarded as 'apparent' parameters, since it cannot be excluded that proton-binding sites with different p*K*-values are involved. However, this cannot be resolved in the framework of the present analysis.

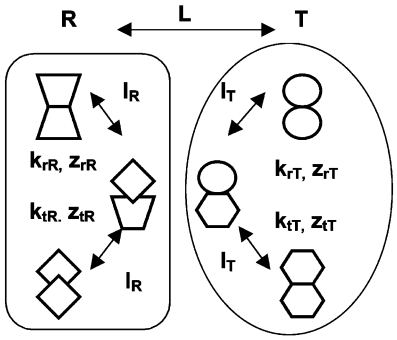

Fig. 1. Nested-MWC-model. The native 2×12-mer can adopt two different overall quaternary structures, *R* and *T*. The equilibrium between these is given by the allosteric constant $L=[T]/[R]$. The two 12-mers form also allosteric units, whose subunits can adopt one of two possible conformations: *rT* and *tT* within the *T* state, *rR* and *tR* within the *R* state. The conformational equilibria are given by the respective allosteric constants: $lR=[tR]/[rR]$ for the transition within the *R* state and $lT=[tT]/[rT]$ within the *T* state. In all cases the allosteric constants describe the ratio of the unliganded forms [26]. Each of the four possible conformations is characterised by an oxygen-binding constant $k_{\alpha\beta}$ and an average proton-binding constant $z_{\alpha\beta}$, $\alpha\beta=rR$, *tR*, *rT* and *tT*.

3.2. Saturation function for oxygen- and proton-binding

The saturation degree with respect to oxygen ($\bar{x}$) and with respect to protons ($\bar{y}_{\mathrm{allo}}$) is given by the following relations [32]:

$$\bar{x}=\frac{\partial \ln P}{24\partial \ln x} \quad \bar{y}_{\mathrm{allo}}=\frac{\partial \ln P}{24m\partial \ln y} \tag{3}$$

When oxygen-binding curves with a constant concentration of free effector are analysed, the effector binding polynomials ($Q_{\alpha\beta}$) are constant, and can therefore be included into the allosteric equilibrium constants, yielding apparent, effector-concentration dependent allosteric equilibrium constants. Then, the binding polynomial relevant

for the description of the oxygen-binding data is given by

$$P=(\mathrm{P}rR^{12}+lR^{\mathrm{app}}PtR^{12})^2 + \Lambda^{\mathrm{app}}(\mathrm{P}rT^{12}+lT^{\mathrm{app}}PtT^{12})^2 \quad (4)$$

$$lR^{\mathrm{app}}=lR^{oo}\frac{QtR^{12m}}{QrR^{12m}} \quad lT^{\mathrm{app}}=lT^{oo}\frac{QtT^{12m}}{QrT^{12m}}$$

$$\Lambda^{\mathrm{app}}=\Lambda^{oo}\frac{QrT^{24m}}{QrR^{24m}}$$

The index '*oo*' at the allosteric equilibrium constants indicates that these are the values in absence of oxygen and protons. Since no data in absence of protons are available, for practical reasons, pH 7.8 was chosen as reference state and indexed '*o*'. The allosteric equilibrium constants at any other pH value are given by

$$lR=lR^{o}\left(\frac{QtR}{QrR}\frac{QrR,o}{QrR,o}\right)^{12\mathrm{m}} \quad lT=lT^{o}\left(\frac{QtT}{QrT}\frac{QrT,o}{QtT,o}\right)^{12\mathrm{m}}$$

$$\Lambda=\Lambda^{o}\left(\frac{QrT}{QrR}\frac{QrR,o}{QrT,o}\right)^{24\mathrm{m}} \quad (5)$$

$$Q_{\alpha\beta,o}=1+z_{\alpha\beta}[H^+]_{\mathrm{pH\ 7.8}} \quad \alpha\beta=tT,\ rT,\ tR,\ rR$$

The analysis of oxygen-binding curves in (non-buffered) Ringer-solution was performed based on Eq. (4). It was assumed that the values of $Q_{\alpha\beta}$ are constant during oxygenation. Indeed, the change in pH is so small that any influence on the value of the allosteric equilibrium constants can be neglected. The small change in pH is a consequence of the large buffering capacity of hemocyanin due to additional, non-allosteric proton-binding sites.

3.3. Inclusion of non-allosteric proton-binding sites

The change in average proton affinity of hemocyanin in response to oxygen binding leads to a redistribution of the total amount of protons between the allosteric binding sites, the non-allosteric buffering sites and the free protons in solution. The only quantity, which is available experimentally, is the free proton concentration. Therefore, in order to analyse the measured change in free proton concentration $[H_\mathrm{f}]$ due to change in oxygen partial pressure, a function of the form $[H_\mathrm{f}]=f(p\mathrm{O}_2)$ is needed. Mass balance for protons leads to the following equation

$$[H_{\mathrm{tot}}]=[H_f]+24[Hc]\{m\times\bar{y}_{\mathrm{allo}}+b\times\bar{y}_{\mathrm{buff}}\} \quad (6)$$

Here, the saturation degree of the allosteric proton-binding sites is given by $\bar{y}_{\mathrm{allo}}$ and is a function of both $[H_\mathrm{f}]$ and $p\mathrm{O}_2$. The saturation degree of the buffering proton-binding sites is denoted by $\bar{y}_{\mathrm{buff}}$ and is a function of $[H_\mathrm{f}]$ only. The concentration of 24-meric hemocyanin is given by $[Hc]$. Each subunit contains m allosteric binding sites and b buffering binding sites. The total proton concentration $[H_{\mathrm{tot}}]$ is not known a priori, but can be substituted by the mass balance (Eq. (6)) in absence of oxygen. In absence of oxygen, the proton concentration is $[H_{\mathrm{fo}}]$ and the saturation degree with respect to protons is denoted by $\bar{y}_{\mathrm{allo},o}$ and $\bar{y}_{\mathrm{buff},o}$, respectively. However, Eq. (6) still cannot be rearranged into a algebraic function $[H_\mathrm{f}]=f(p\mathrm{O}_2)$ in the present form. Therefore, the saturation degree of the buffering proton-binding sites is approximated by a Taylor-series. This approximation is allowed, since the experimental change in free proton concentration upon change in oxygen concentration is very small. Thus, one may write

$$\bar{y}_{\mathrm{buff}}=\bar{y}_{\mathrm{buff},o}+\frac{K_{\mathrm{buff}}}{(1+K_{\mathrm{buff}}[H_{fo}])^2}\Delta[H_f] \quad (7)$$

$$\Delta[H_f]=[H_f]-[H_{fo}]$$

$$\bar{y}_{\mathrm{buff},o}=\frac{K_{\mathrm{buff}}[H_{fo}]}{1+K_{\mathrm{buff}}[H_{fo}]}$$

Using this approximation for $\bar{y}_{\mathrm{buff}}$, substituting $[H_{\mathrm{tot}}]$ and rearranging Eq. (6) yields the following expression:

$$\Delta[H_f] = -Q_{\text{buff}}\Delta\bar{y} \quad \Delta\bar{y}_{\text{allo}} = \bar{y}_{\text{allo}} - \bar{y}_{\text{allo},o}$$

$$Q_{\text{buff}} := \frac{24m[Hc]}{1+\Phi\times 24m[Hc]}$$

$$\Phi := b\frac{K_{\text{buff}}}{\left(1+K_{\text{buff}}[H_{fo}]\right)^2} \tag{8}$$

Thus, the measured change in free proton concentration corresponds to the change in concentration of protons bound to the allosteric binding sites, reduced by a factor Q_{buff}. This factor depends on the hemocyanin concentration, pH at the beginning of the experiment $[H_{\text{fo}}]$, buffering affinity K_{buff} and number of buffering binding sites b.

When Eq. (8) is fitted to the data, a strong correlation between the values for the number of proton-binding sites m and the values for the proton-binding constants (*ztT*, *ztR*, *zrR* and *zrT*) is observed. Thus, the analysis was performed for different values of m (Fig. 3). The most likely value for m was then determined by comparison with the results from analysing the total buffering capacity of hemocyanin in the oxygenated state for different values of m.

3.4. Analysis of total buffering capacity

In order to determine the overall buffering capacity under oxygenated conditions, a solution of hemocyanin at given starting pH was titrated with NaOH and the corresponding change in pH was measured. For each equivalent of $[OH^-]$ ions, the same amount of protons is removed, thus yielding

$$-\Delta[OH^-] = \Delta[H]_{\text{bound}}$$

$$= \left[m\Delta\bar{y}_{\text{allo}} + b\Delta\bar{y}_{\text{buff}}\right]24[Hc] \tag{9}$$

For the data analysis, the contribution of $\Delta\bar{y}_{\text{allo}}$ was calculated based on the values for the allosteric binding constants obtained in the analysis of the proton release and uptake. This was performed for different stoichiometries ($m = 1, 2, 5$) and the non-allosteric proton-binding parameters K_{buff} and b were fitted to the titration data for each value of m.

The fitting procedures were performed employing the non-linear-regression package in SIGMAPLOT (SSPS, Chicago, IL).

4. Results

In order to understand the complex interaction of spider hemocyanin with protons and oxygen, oxygen-binding curves obtained at pH values of 7.3, 7.6 and 7.8 and the change in the pH value upon changes in oxygen partial pressure at pH 7.4, 7.6 and 8.0 were analysed based on the Nested-MWC-model. The four conformations of the Nested-MWC-model are characterised by four proton-binding constants (*ztT*, *ztR*, *zrR* and *zrT*), the stoichiometry for proton binding (m) per subunit, four oxygen-binding constants (*ktT*, *ktR*, *krR* and *krT*) and three allosteric equilibrium constants (see also Fig. 1). The non-allosteric proton-binding behaviour is characterised by an average binding constant K_{buff} and the corresponding stoichiometry b per subunit. The non-allosteric proton binding was explicitly included into the allosteric model describing proton release and uptake (Eq. (8)). By a stepwise, simultaneous analysis of the six data sets in Fig. 2, it was possible to determine a set of binding parameters which are valid for both types of data sets as summarized in Table 1. The calculated curves based on these parameter values are also depicted in Fig. 2. Obviously, the Nested-MWC-model is able to describe both proton-binding and oxygen-binding behaviour of hemocyanin from *E. californicum* in Ringer-solution. The values for the oxygen-binding constants *krR* and *krT* were set constant to the values obtained in the analysis of the binding data in presence of TRIS-buffer [33] ($krT = 3.5$ Torr^{-1} and $krR = 2$ Torr^{-1}). These values had to be set constant, because they were not well defined by the present data. The remaining two oxygen-binding constants and the allosteric equilibrium constants were well defined, when both type of data sets were used for the analysis. The oxygen-binding data alone, or the data for proton release and uptake alone are not sufficient to determine all the allosteric binding parameters.

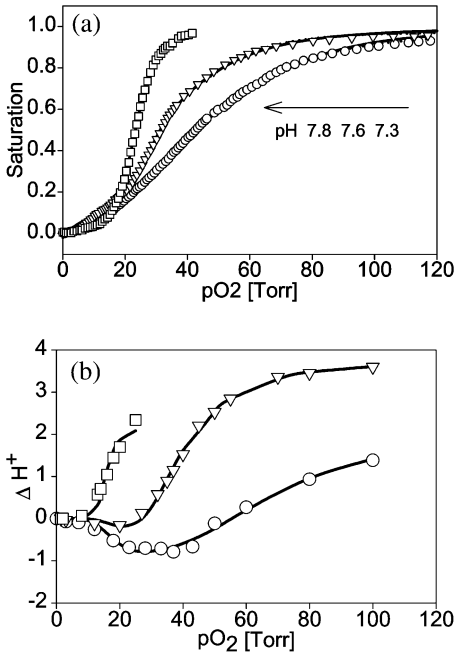

Fig. 2. Proton- and oxygen-binding. *Panel A*: pH dependence of oxygen-binding curves in Ringer-solution. pH values: 7.3 (circles), 7.6 (triangles) and pH 7.8 (squares). *Panel B*: The change in pH upon oxygenation was determined in Ringer-solution at pH values 7.4 (circles), 7.6 (triangles) and 8.0 (squares), data are as shown in [29]. The lines correspond to fits based on the values in the range as given in Tables 1 and 2 ($m=2$ non-allosteric proton-binding sites).

The stoichiometry of proton binding m cannot be determined unambiguously based on the analysis of these six data sets. Thus, the analysis was performed for a range of values ($m=1$, 2, 5, 10) by fitting the corresponding equation to the data. The result is shown in Fig. 3. The value for each

Table 2
Results of analysis of total buffering capacity

	$m=1$	$m=2$	$m=5$	$m=10$
K_{buff}	0.008	0.006	0.003	<0.00026
B	11	10.8	9	>18

The errors for K_{buff} are approximately 30%, for b approximately 10%. For $m=10$, K_{buff} and b are correlated, thus only upper and lower limits can be given.

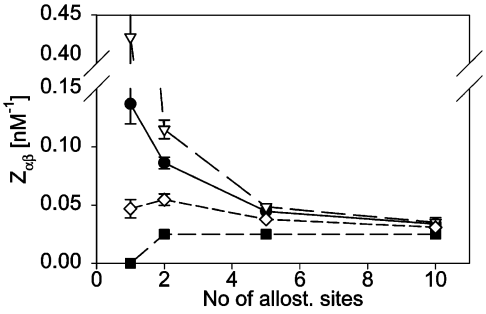

Fig. 3. Dependence of the proton-binding affinity on the stoichiometry. Since the value of the proton-binding stoichiometry (m) cannot be determined based on the data set shown in Fig. 2, the analysis was performed for different values of m. The values for the protein affinity strongly depend on m. All other parameters depend only weakly on m (not shown).

binding constant *ztT*, *ztR*, *zrR* and *zrT* decreases with increasing stoichiometry m. However, the order of affinity of the four conformations is independent on the stoichiometry: $zrT<zrR<ztT<ztR$. The conformation with the lowest affinity for protons is conformation *rT*. The values given for the affinity of this conformation are upper values, since no lower limit could be determined. The upper value was defined as the value,

Table 1
Allosteric equilibrium and binding constants for the oxygen- and proton-binding of hemocyanin from *E. californicum*

Allosteric equilibrium constants		Oxygen-binding constants		Proton-binding constants (nM^{-1})		pK
$\log lR^o$	17.9 ± 0.2	*ktT*	0.008 ± 0.002	*ztT*	0.080 ± 0.005	7.9
$\log \Lambda^o$	-2.5 ± 0.1	*ktR*	0.035 ± 0.01	*ztR*	0.12 ± 0.01	8.1
$\log lT^o$	21.9 ± 0.5	*krT*	3.5[§]	*zrT*	<0.02	<7.3
$\log L^*$	5.2 ± 0.6	*krR*	2[§]	*zrR*	0.055 ± 0.005	7.7

The values are based on $m=2$ allosteric proton-binding sites per subunit. Errors are based on the variation of the values in the different steps of analysis. (*L calculated from Λo, lTo, lRo; [§]set constant to values as found in presence of TRIS [26]).

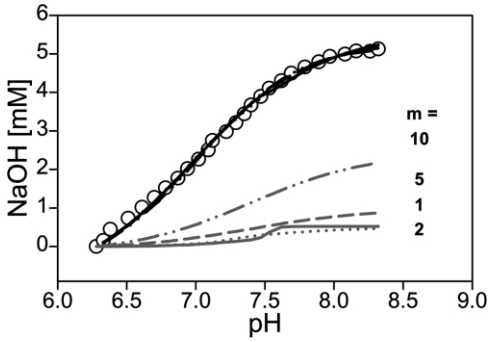

Fig. 4. Buffering capacity of hemocyanin in Ringer-solution. The buffering capacity was determined based on titration of an oxygenated hemocyanin solution (open circles). The data were analysed as described in the text for different values of proton-binding stoichiometry (m), yielding a buffering constant and the number of buffering proton-binding sites per subunit for each value of m (Table 2). The total buffering is shown in black. The contribution of the allosteric binding sites based on the Nested-MWC-model are shown in grey for each value of m.

which led to a decrease in the quadratic regression coefficient of 0.0002. The values of the other three proton-binding constants did not strongly depend on zrT. The buffering binding constant and the total number of non-allosteric binding sites (b) were only weakly depending on m in this analysis: $b = 17 \pm 5$ and $K_{\text{buff}} = 0.033 \pm 0.009$ nM^{-1}, corresponding to a pK of 7.5. The values of the oxygen-binding constants and the allosteric equilibrium constants did not depend on m.

In order to get an estimate of the value for m, the buffering capacity of hemocyanin from *E. californicum* was measured directly under oxygenated conditions and analysed based on Eq. (9) with fixed values for m, yielding values for K_{buff} and b for each value of m. Data, fitted curves and the contribution of the allosteric sites to the buffering capacity are depicted in Fig. 4. The value for K_{buff} decreased with increasing m. The comparison of these values for K_{buff} with those obtained before (Table 1) supports small values for m, yielding $K_{\text{buff}} = 0.008 \pm 0.003$ nM^{-1}. The number of buffering binding sites per subunit is approximately 11 ± 1 ($m = 1, 2$) as inferred from the direct measurement and approximately 17 ± 5 as indicated by the analysis of proton release data, and agree within the error ranges.

5. Discussion

The regulation of hemocyanins by protons and, depending on the species, a variety of other organic and inorganic effectors, is a well-known effect. The analysis of oxygen-binding curves at different pH values in buffered solutions indicated, for a number of hemocyanins, that concerted models such as the MWC-model or the Nested-MWC-model are suitable descriptions for the cooperative and allosteric binding behaviour respecting the hierarchy in structure [21,23–28]. In these models, the protein can adopt different conformations, which differ in their affinity for ligands and effectors. These conformations are responsible for the cooperative and allosteric properties, and therefore for the correct functioning of the oxygen carrier. In order to understand the mechanism of cooperative and allosteric regulation, these conformations need to be characterised in terms of their ligand- and effector-binding properties. While the oxygen-binding affinity of the different conformations was determined for *E. californicum* and a number of other hemocyanins, reports on the affinity of effectors are only available for organic effectors such as urate [7,11,19]. In none of these studies, binding of an effector is included into an allosteric model for cooperativity. However, this strategy would provide a stringent test of the applicability of concerted models.

Hemocyanin from *E. californicum* is one of the best-investigated hemocyanins in terms of oxygen-binding properties. It has been shown that the Nested-MWC-model is well suited to describe the oxygen-binding properties in TRIS-buffered solution [26]. However, it turned out that TRIS acts as an effector [33]. The only physiological effectors identified so far are protons and possibly water [34]. In this study, I present an analysis of the cooperative oxygen binding of this hemocyanin including the allosteric and non-allosteric binding of protons.

5.1. Oxygen- and proton-binding

Both types of data sets analysed in this study (oxygen- and proton-binding curves, obtained in

Ringer-solution) can be described by a common set of oxygen-binding, proton-binding and allosteric equilibrium constants. The set of oxygen-binding constants obtained are in good agreement with the values determined for TRIS- and HEPES-buffer. This result supports the applicability of the Nested-MWC-model for physiologically relevant conditions as in Ringer-solution. Furthermore, the explicit inclusion of proton-binding parameters into the analysis presents a much more stringent test of the applicability of the Nested-MWC-model than the analyses employed so far, where no restrictions for the values of the allosteric equilibrium constants were imposed.

One might consider simpler models for the description of the function of hemocyanin from *E. californicum* with a smaller number of independent parameters. The simplest concerted model (the MWC-model [35]) was ruled out already [25,26,36]. Models that have a degree of complexity between the MWC-model and the Nested-MWC are the hybrid model [27,37] and the three-state MWC-model [38]. The three-state MWC-model is characterised by three conformations (T, S and R) that are available for the allosteric unit. In order to check whether the data presented here can be described by this model as well, the analysis was performed for an allosteric unit consisting of 24 subunits. The choice of $n=24$ was based on a detailed investigation of the binding behaviour of the 24-meric native molecule in comparison to intermediates (19- , 12- , 7- and 6-mers) which showed that full cooperativity is established only for the native 24-meric molecule [39]. The pH dependence of the affinity of oxygen binding at very low and very high saturation (K_1 and K_n in the Hill-plot) showed independently of any model that the maximal affinity of the 24-meric molecule was $K_n=3.4$ Torr^{-1} [26]. Thus, the highest affinity in the three-state model (K_R) was constrained to this value. Indeed, the six curves in Fig. 2 can be analysed reasonably well based on this approach. In order to check whether the three-state model is applicable in general to this hemocyanin, data obtained at different Glycine-concentrations were also re-analysed. These data could be analysed based on the Nested-MWC-model in full agreement with all other data available [34]. When these data were analysed based on the three-state model without any constraints, an agreement comparable with that found for the Nested-MWC-model was observed. However, the highest affinity ($K_R=0.71\pm0.11$ Torr^{-1}) was too low to be in agreement with the data obtained at high pH values ($K_n=3.4\pm0.2$ Torr^{-1}). When K_R was constrained to this value in the analysis, the sum of the squared residuals was approximately twice as large as that for the Nested-MWC-model. Furthermore, the oxygen affinity of the intermediate affinity (K_S) did not agree for the two data sets ($K_S=0.087\pm0.01$ Torr^{-1} for the data with Glycine and $K_S=0.044\pm0.01$ Torr^{-1} for the data in Ringer-solution). Thus, the three-state model seems to be applicable for sub-sets of the data available for oxygen binding of hemocyanine from the spider from *E. californicum*, but not for all data simultaneously. In contrast, several observation points towards the Nested-MWC-model as a suitable description of cooperative and allosteric binding properties of this hemocyanin. An analysis of the isolated 12-meric molecules showed that the values for K_1 and K_n in the Hill-plot are very similar as those found for the R-state of the native 24-mer. Furthermore, CO and oxygen binding and the competition between these two ligands could well be analysed based on the Nested-MWC-model [25], with essentially the same set of four oxygen-binding constants as for the pH dependence in TRIS [26], the dependence on TRIS- and Glycine-concentration at pH 7.8 [33,34] and the pH dependence in Ringer-solution including proton release and uptake.

On the basis of the present analysis, for the first time estimates for the proton affinity of the different conformations of a hemocyanin are given. The data for proton release and uptake of spider hemocyanin showed a remarkable non-monotonous response to a change in oxygen saturation in contrast to vertebrate hemoglobin, where a linear response was reported [30]. This behaviour is reflected in the order of affinities for protons for the different conformations: $zrT<zrR<ztT<ztR$ (Table 1). This order in the proton affinity of the four conformations is obtained regardless which stoichiometry for proton binding was assumed. The proton-binding affinities of the four confor-

mations do not cover a broad range (0.02–0.12 nM^{-1}, pH 7.3–8.1, Table 1), giving a factor of approximately 6 between the lowest and the highest affinity. For comparison: the factor between the lowest and highest oxygen affinity is approximately 300.

A total amount of approximately 12–19 proton-binding sites per subunit are present: 1–2 allosteric and 11–17 non-allosteric sites. The average binding affinity for the buffering binding sites is between 0.008 and 0.03 nM^{-1}, corresponding to a p*K* of 6.9–7.5. The range of p*K* values for all types of proton-binding sites indicates that only histidines are involved in proton binding. Indeed, spider hemocyanin offers approximately 30 histidine residues per subunit mostly located on the surface. When the sequence obtained by [40] is modelled on the crystal structure of *L. polyphemus*, approximately 50 histidines of the hexamer are classified as medium or well exposed (based on Swiss-PDB-Viewer). Thus, a large number of proton-binding sites is not contradicted by the sequence data.

The major fraction of proton-binding sites are non-allosteric, buffering binding sites. The buffering capacity of purified hemocyanin is approximately 3 mM per pH at a hemocyanin concentration of 40 mg ml^{-1}. In contrast, values reported for diluted hemolymph are up to twofold higher and apparently did not correlate with the total protein concentration [41]. Thus, in the hemolymph additional protein buffering components are present. The most likely candidate is the non-respiratory protein. This protein is found in the hemolymph of *E. californicum* with varying concentrations up to 20% of the total protein content. Its function apart from a possible role in proton buffering is not yet known.

5.2. Physiological considerations

Since now the allosteric parameters in physiological Ringer-solution are available, the fraction of molecules in each of the four conformations *tT*, *tR*, *rR* and *rT* can be calculated for various physiological conditions. This is shown in Fig. 5, where the conformational distribution at pH 7.5 (animal at rest, Fig. 5a) and pH 7.0/pH 7.25 (locomotion and recovery, Fig. 5b) is shown. Venous and arterial oxygen pressure under rest and recovery as determined by [16] are also indicated.

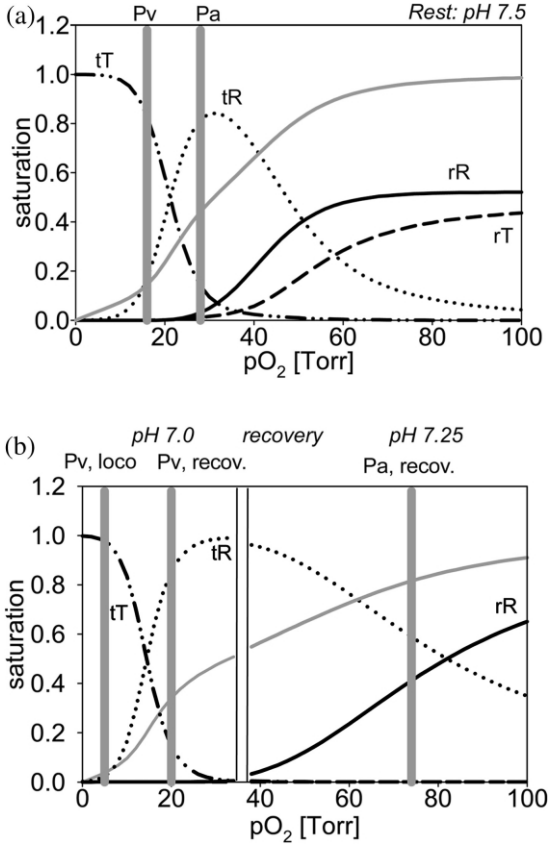

Fig. 5. pH dependence of the conformational distribution. *Panel A*: resting conditions, pH 7.5; *Panel B*: after locomotion (left side, pH 7.0) and at recovery (right side, pH 7.5). The grey lines correspond to the total saturation with respect to oxygen. The black line corresponds to the conformations as indicated. The grey bars indicate oxygen partial pressure (venous p_v and arterial p_a) under conditions as given in the figures.

Under rest, where hemocyanin does not transport much oxygen [42], only conformations *tT* and *tR* are present in significant amounts (Fig. 5a). The two remaining conformations *rR* and *rT* would be populated only at higher oxygen pressures, which seem not to be of importance in vivo at rest.

After locomotion, the pH value drops to approximately 7 in venous regions (left part in Fig. 5b)

and to approximately 7.25 in arterial regions (right part in Fig. 5b). The arterial pO_2 increases directly after locomotion to approximately 74 Torr, allowing a significant saturation of hemocyanin despite the lowered pH value. The venous pO_2 drops to approximately 5 Torr shortly after locomotion and increases then to approximately 20 Torr [16]. Under these conditions hemocyanin can transport oxygen from the lungs to the tissue, since the saturation degree drops from approximately 80 to 40% between 20 and 74 Torr. Conformation *rR* is populated mainly in the lung, whereas conformation *tR* dominates at the tissue.

Conformation *tR* has the highest affinity for protons, and is populated over a broad pO_2-range. Thus, this conformation might play a role in the transport of protons from the tissue, where protons accumulate due to L-lactate formation, to the lungs, where the pH can be regulated by CO_2-emmission [43]. In contrast, conformation *rT* is not utilized under any of the afore mentioned conditions. However, when the pH is further increased, this conformation becomes increasingly dominant. Thus, under conditions, where the animal experiences alkalosis, conformation *rT* might become important.

Acknowledgments

I would like to thank Dr Heinz Decker for his support and discussion and Dr Reinhard Sterner (University of Köln) for supplying experimental data. This work was supported by the DFG, the MWFZ Mainz and the NMFZ Mainz.

References

[1] J. Markl, H. Decker, Molecular structure of the arthropod hemocyanins, Adv. Comp. Environ. Physiol. 13 (1992) 319–376.
[2] K.E. van Holde, K.I. Miller, Haemocyanins, Q. Rev. Biophys. 15 (1982) 1–129.
[3] K.E. van Holde, K.I. Miller, Hemocyanins, Adv. Protein Chem. 47 (1995) 1–81.
[4] K.E. van Holde, K.I. Miller, E. van Olden, Allostery in very large molecular assemblies, Biophys. Chem. 86 (2000) 165–172.
[5] R.A. Graham, A model for L-lactate binding to cancer magister hemocyanin, Comp. Biochem. Physiol. B 81 (1985) 885–887.
[6] H. Hartmann, B. Lohkamp, N. Hellmann, H. Decker, The allosteric effector L-lactate induces a conformational change of 2×6-meric lobster hemocyanin in the oxy state as revealed by small angle X-ray scattering, J. Biol. Chem. 276 (2001) 19954–19958.
[7] N. Hellmann, E. Jaenicke, H. Decker, Two types of urate binding sites on hemocyanin from the crayfish *Astacus leptodactylus*: an ITC study, Biophys. Chem. 90 (2001) 279–299.
[8] B.A. Johnson, J. Bonaventura, C. Bonaventura, Determination of L-lactate binding stoichiometry and differences in allosteric interactions of structurally distinct homohexamers from Panulirus interruptus hemocyanin, Biochim. Biophys. Acta 916 (1987) 376–380.
[9] F. Lallier, J.P. Truchot, Hemolymph oxygen transport during environmental hypoxia in the shore crab, *carcinus meanas*, Respir. Physiol. 77 (1989) 323–336.
[10] B.R. McMahon, Respiratory and circulatory compensation to hypoxia in crustaceans, Respir. Physiol. 128 (2001) 349–364.
[11] M.A. Menze, N. Hellmann, H. Decker, M.K. Grieshaber, Binding of urate and caffeine to hemocyanin of the lobster *Homarus vulgaris* (E.) as studied by isothermal titration calorimetry, Biochemistry 39 (2000) 10806–10811.
[12] S. Morris, C.R. Bridges, M.K. Grieshaber, A new role for uric acid: modulator of haemocyanin affinity in crustaceans, J. Exp. Zool. 235 (1985) 135–139.
[13] L. Hagerman, B. Vismann, Modulators of haemocyanin oxygen affinity in the hypoxia- and sulphide-tolerant Baltic isopod *Saduria entomon* (L.), J. Comp. Physiol. B 171 (2001) 695–699.
[14] C.R. Bridges, Modulation of haemocyanin oxygen affinity: properties and physiological implications in a changing world, J. Exp. Biol. 204 (2001) 1021–1032.
[15] H.D. Ellerton, N.F. Ellerton, H.A. Robinson, Hemocyanin—a current perspective, Prog. Biophys. Mol. Biol. 41 (1983) 143–248.
[16] D. Angersbach, Oxygen transport in the blood of the tarantula *Eurypelma californicum*: pO_2 and pH during rest, activity and recovery, J. Comp. Physiol. B 123 (1978) 113–125.
[17] O. Brix, G. Lykkeboe, K. Johansen, The significance of the linkage between the Bohr and Haldane effects in cephalopod bloods, Respir. Physiol. 44 (1981) 177–186.
[18] B. Giardina, S.G. Condo, O. Brix, The interplay of temperature and protons in the modulation of oxygen binding by squid blood, Biochem. J. 281 (Pt 3) (1992) 725–728.
[19] A. Nies, B. Zeis, C.R. Bridges, M.K. Grieshaber, Allosteric modulation of haemocyanin oxygen-affinity by L-lactate and urate in the lobster *Homarus vulgaris*. II. Characterization of specific effector binding sites, J. Exp. Biol. 168 (1992) 111–124.
[20] K.I. Miller, C.P. Mangum, An investigation of the nature of Bohr, Root, and Haldane effects in Octopus dofleini hemocyanin, J. Comp. Physiol. B 158 (1988) 547–552.

[21] F. Arisaka, K.E. Van Holde, Allosteric properties and the association equilibria of hemocyanin from *Callianassa californiensis*, J. Mol. Biol. 134 (1979) 41–73.
[22] A. Klarman, N. Shaklai, E. Daniel, Oxygen binding by hemocyanin from *Levantina hierosolima*. I. Exclusion of subunit interactions as a basis for cooperativity, Biochemistry 14 (1975) 102–104.
[23] P.R. Connelly, C.R. Johnson, C.H. Robert, H.J. Bak, S.J. Gill, Binding of oxygen and carbon monoxide to the hemocyanin from the spiny lobster, J. Mol. Biol. 207 (1989) 829–832.
[24] E. Dainese, P. Di Muro, M. Beltramini, B. Salvato, H. Decker, Subunits composition and allosteric control in *Carcinus aestuarii* hemocyanin, Eur. J. Biochem. 256 (1998) 350–358.
[25] H. Decker, P.R. Connelly, C.H. Robert, S.J. Gill, Nested allosteric interaction in tarantula hemocyanin revealed through the binding of oxygen and carbon monoxide, Biochemistry 27 (1988) 6901–6908.
[26] H. Decker, R. Sterner, Nested allostery of arthropodan hemocyanin (*Eurypelma californicum* and *Homarus americanus*). The role of protons, J. Mol. Biol. 211 (1990) 281–293.
[27] B.A. Johnson, C. Bonaventura, J. Bonaventura, Allostery in Callinectes sapidus hemocyanin: cooperative oxygen binding and interactions with L-lactate, calcium, and protons, Biochemistry 27 (1988) 1995–2001.
[28] M. Brouwer, B. Serigstad, Allosteric control in *Limulus polyphemus* hemocyanin: functional relevance of interactions between hexamers, Biochemistry 28 (1989) 8819–8827.
[29] R. Sterner, H. Decker, Inversion of the Bohr effect upon oxygen binding to 24-meric tarantula hemocyanin, Proc. Natl. Acad. Sci. USA 91 (1994) 4835–4839.
[30] M.L. Johnson, B.W. Turner, G.K. Ackers, A quantitative model for the cooperative mechanism of human hemoglobin, Proc. Natl. Acad. Sci. USA 81 (1984) 1093–1097.
[31] J. Markl, A. Savel, H. Decker, B. Linzen, Hemocyanins in spiders, IX. Homogeneity, subunit composition and the basic oligomeric structure of *Eurypelma californicum* hemocyanin, Hoppe Seylers Z. Physiol. Chem. 361 (1980) 649–660.
[32] J. Wyman, S.J. Gill, Binding and Linkage, University Science Books, 1990.
[33] R. Sterner, K. Bardehle, R. Paul, H. Decker, Tris: an allosteric effector of tarantula haemocyanin, FEBS Lett. 339 (1994) 37–39.
[34] N. Hellmann, K. Raithel, H. Decker, A potential role of water in allosteric regulation of tarantula hemocyanin', Comp. Biochem. Physiol. A: Mol. Integrative Physiol. 136 (2003) 725–734.
[35] M.A. Wyman, J.P. Changeux, On the nature of allosteric transitions: a plausible model', J. Mol. Biol. 12 (1965) 88–118.
[36] H. Decker, A. Savel, B. Linzen, K.E. Van Holde, A new graphical test for the MWC-model and its application to some hemocyanins, Life Chem. Rep. 1 (Suppl. 1) (1983) 156–251.
[37] M. Brouwer, C. Bonaventura, J. Bonaventura, Analysis of the effect of three different allosteric ligands on oxygen binding by hemocyanin of the shrimp, *Penaeus setiferus*, Biochemistry 17 (1978) 2148–2154.
[38] B. Richey, H. Decker, S.J. Gill, Binding of oxygen and carbon monoxide to arthropod hemocyanin: an allosteric analysis, Biochemistry 24 (1985) 109–117.
[39] A. Savel-Niemann, J. Markl, B. Linzen, Hemocyanins in spiders. XXII. Range of allosteric interaction in a four-hexamer hemocyanin. Co-operativity and Bohr effect in dissociation intermediates, J. Mol. Biol. 204 (1988) 385–395.
[40] R. Voit, G. Feldmaier-Fuchs, T. Schweikardt, H. Decker, T. Burmester, Complete sequence of the 24-mer hemocyanin of the tarantula *Eurypelma californicum*. Structure and intramolecular evolution of the subunits, J. Biol. Chem. 275 (2000) 39339–39344.
[41] R. Paul, B. Bergner, R. Pfeffer-Seidl, H. Decker, R. Efinger, H. Storz, Gas transport in the haemolymph of arachnids I. Oxygen transport and the physiological role of haemocyanin, J. Exp. Biol. 188 (1994) 25–46.
[42] R. Paul, B. Bergner, A. Pfeffer-Seidl, H. Decker, R. Efinger, H. Storz, Gas transport in the haemolymph of arachnids-oxygen transport and the physiological role of haemocyanin, J. Exp. Biol. 188 (1994) 25–46.
[43] J. Wyman, S.J. Gill, Binding and Linkage, University Science Books, 1990.